

CLOUD-CLEAR AIR INTERFACIAL MIXING: ANISOTROPY OF TURBULENCE GENERATED BY EVAPORATION OF LIQUID WATER. LABORATORY OBSERVATIONS AND NUMERICAL MODELLING

Szymon P. Malinowski¹, Mirosław Andrejczuk², Wojciech W. Grabowski³, Piotr Korczyk⁴,
Tomasz A. Kowalewski⁴ and Piotr K. Smolarkiewicz³

¹ Warsaw University, Institute of Geophysics, Warsaw, Poland.

² Los Alamos National Laboratory, Los Alamos, New Mexico, USA.

³ National Center for Atmospheric Research, Boulder, Colorado, USA.

⁴ Institute of Fundamental Technological Research, Polish Academy of Sciences, Warsaw, Poland.

1. INTRODUCTION

The so called "warm rain initiation problem" attracts attention of cloud physicists, turbulence researchers, engineers and meteorologists. It is still uncertain which mechanism is responsible for the formation of drizzle and rain (precipitation) drops. Papers concerning the impact of high-Reynolds-number turbulence on spatial distribution of cloud droplets, their diffusional growth, collisions, and coalescence are published at high rate. Our understanding of particle motion in turbulent flows is based on both theoretical and experimental studies. Recent comprehensive reviews of these efforts can be found in Vaillancourt and Yau (2000), Falkovich et al. (2001), Shaw (2003), and Ghosh et al. (2005).

Unfortunately, properties of cloud turbulence at scales relevant for the interactions between droplets and the air flow have never been documented. In a recent paper by Siebert et al. (2006) the authors were able to study turbulent velocities at scales down to 20 cm. Such a scale is still about two orders of magnitude larger than a typical distance between cloud droplets, which, coincidentally, is also the Kolmogorov microscale for typical levels of cloud turbulence. It follows that far-reaching assumptions have to be made in order to study interaction between cloud dynamics, thermodynamics, and microphysics. Usually it is assumed, that cloud turbulence is generated at large scales (100m or more), it cascades through the inertial range of turbulent eddies down to the Kolmogorov microscale, where it is dissipated. At the smallest scales turbulent velocities are assumed to be isotropic and are described by statistical distributions based on laboratory/wind tunnel/atmospheric boundary layer measurements or direct numerical simulation (DNS). It is also assumed that temperature and humidity are passive scalars, i.e. they do not influence small-scale dynamics through the buoyancy effects.

This paper shows that these assumptions are not always fulfilled. We present results of numerical simulations and laboratory cloud chamber experiments with turbulent mixing between cloudy air and unsaturated clear air at scales down to a fraction of a centimeter. It appears that at these scales turbulence is substantially anisotropic due to the action of buoyancy

forces resulting from evaporation of cloud droplets. In the next section, a theoretical discussion of the problem is provided. Section 3 is devoted to a brief presentation of laboratory experiments. Short description of numerical simulations is given in section 4, and key results are summarized in section 5.

2. THEORETICAL CONSIDERATIONS.

Consider the isobaric entrainment event of environmental air at the cloud top or near cloud edge. Once a parcel of unsaturated environmental air becomes engulfed by saturated cloudy air containing small water droplets, both volumes undergo stirring and filamentation driven by turbulence cascading down from large scales. Thermodynamic processes (e.g., phase change) and chemical reactions occur at the interface separating these filaments (see e.g. Broadwell and Breidenthal 1982; Grabowski 1993; Malinowski and Zawadzki, 1993). There are two transport mechanisms acting across this interface:

1) molecular diffusion of water vapor and heat, which is independent on the orientation of the interface;

2) gravitational sedimentation of cloud droplets from cloud to clear air filaments (liquid water transport), which is sensitive to the interface orientation.

Both mechanisms lead to partial or complete evaporation of cloud droplets. Evaporative cooling in a narrow sheet at the interface results in density changes, and consequently buoyancy differences at small scales. Vertical motions are usually correlated with buoyancy forces, which influence the turbulent kinetic energy (TKE) through the buoyancy production term $\langle w'B' \rangle$ (see a turbulence textbook or the appendix in Andrejczuk et al. 2006). Here w' stands for the vertical component of the velocity fluctuation, B' is the buoyancy fluctuation, and $\langle \rangle$ depicts volume averaging. Note that TKE production due to buoyancy is correlated with vertical motions. This means that the vertical direction is privileged and there is no isotropy.

In a stationary isotropic turbulence, TKE decreases with spatial scale according to the $-5/3$ law. It follows that only a tiny fraction of TKE is contained in scales close to the dissipation (Kolmogorov) scale, which in most atmospheric flows is around one millimeter. Scales from a fraction of millimeter to a few centimeters are crucial for the interactions between turbulence and cloud droplets, droplet evaporation, droplet spacing etc. These are scales at which processes at the interface

*Corresponding author address: Szymon P. Malinowski, Warsaw University, Institute of Geophysics, ul. Pasteura 7, 02-093 Warsaw, Poland; e-mail: malina@fuw.edu.pl

between cloudy and clear air filaments occur. Even small work due to buoyancy can be enough to influence TKE at small scales.

Such cloud-clear air mixing processes have been investigated in a series of numerical simulations discussed in Andrejczuk et al. (2004, 2006) and in the laboratory experiments inside a cloud chamber (Malinowski et al. 1998; Banat and Malinowski 1999; Malinowski and Jaczewski 1999; Korczyk et al. 2006). In the following we compare results of the laboratory and numerical studies with the emphasis on distribution functions of horizontal and vertical turbulent fluctuations, and on other small scale features of investigated flows.

3. LABORATORY EXPERIMENTS.

An experimental chamber (1.0m x 1.0m x 1.8m) and the method of generation of the artificial cloud (consisting of droplets with mean diameter of about $6\mu\text{m}$) is described in Korczyk et al. (2006). The negatively buoyant cloudy plume enters the chamber through the round opening at the upper wall with velocity of about 10cm/s. The plume accelerates due to its negative buoyancy to about 20cm/s in the middle of the chamber. Liquid water content of the plume is usually more than 10g/kg, its temperature is around 25°C, similar to the temperature of unsaturated air in the chamber. Relative humidity of the clear air inside the chamber is typically around 60%. The plume descends while mixing with the environment, creating complicated, constantly evolving structures (eddies, filaments, etc.).

Illumination of the chamber interior with 1.2mm thick sheet of laser light allows imaging the planar cross section through the scene with a high-resolution CCD camera. An example image from the experiment, covering area of about $9 \times 6 \text{cm}^2$ is presented in Fig.1.



Fig.1. An example image from the cloud chamber. Dark pixels are occupied with cloud droplets. Image covers area of $\sim 9 \times 6 \text{cm}^2$

Inspection of the image reveals fine structures created in the process of turbulent mixing of the cloudy plume with its unsaturated environment. One pixel in this image corresponds to the volume of about $69 \times 69 \mu\text{m}^2$ in the plane of the light sheet and 1.2mm

deep. Such elementary volumes occupied by droplets are represented by dark pixels in the image, bright pixels correspond to volumes with no droplets.

Identification of patterns in the two consecutive images separated by a known time interval allows determination of two components of the velocity. This technique is widely adopted in experimental fluid dynamics under name of Particle Image Velocimetry (PIV). A precise multiscale PIV algorithm, identifying first motions of large structures and then displacements within these structures, has been developed for this experiment. Its details are given in Korczyk et al. (2006). An example of the retrieved two components of turbulent velocity fluctuations is shown in Fig. 2.

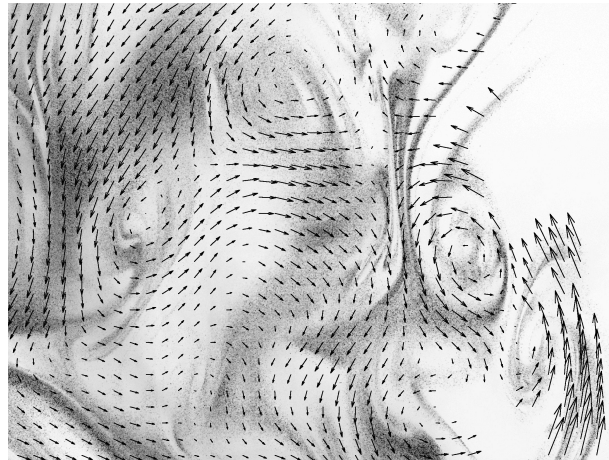


Fig.2. An example of two-dimensional retrieval of turbulent velocity fluctuations obtained from the pair of consecutive images by means of PIV technique. Mean motion has been removed.

Application of PIV algorithm allows estimating the two components of velocity vector in the plane of the image with spatial resolution of about 0.07mm, i.e. an order of magnitude better than the Kolmogorov microscale, calculated directly from the measurements as approximately 0.76mm.

Three series of experiments with slightly varying thermodynamical conditions inside the chamber have been performed. In each series, at least 500 pairs of frames (tens of thousands of vectors in each frame) have been analyzed in order to retrieve properties of turbulent velocity fluctuations. Combined statistics of these fluctuations in horizontal (u') and vertical (w') directions are presented in Fig.3 and summarized in Table 1.

TABLE 1. Distribution of horizontal (u') and vertical (w') turbulent velocity fluctuations in the experiment.

	Standard deviation [cm/s]	Skewness	Kurtosis
u'	5.4	-0.01	3.2
w'	8.0	-0.2	3.1

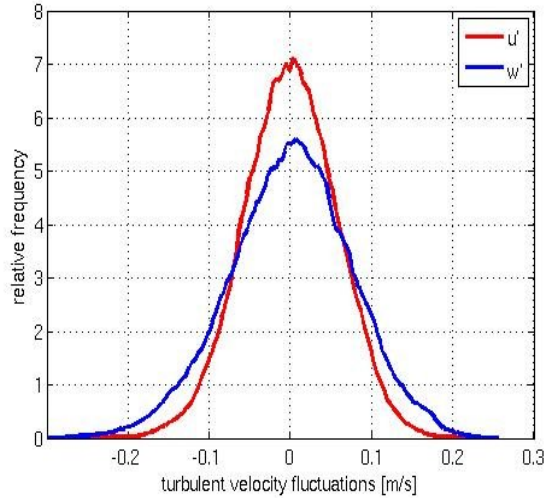


Fig. 3. Composite distribution of horizontal (red) and vertical (blue) turbulent velocity fluctuations from three series of measurements.

It is evident that the distribution of the vertical turbulent velocity fluctuations is wider and has longer tails than the distribution of horizontal fluctuations. Calculated skewness and kurtosis indicate that both distributions are close to the Gaussian (normal). A clear indicator of the anisotropy is the ratio of the root mean square of turbulent fluctuations: $\langle w'^2 \rangle / \langle u'^2 \rangle$, which is around 2.2. It has to be stressed that there is no difference whether averaging is performed on all the experimental data, on consecutive series, and even on individual scenes (i.e., pairs of frames). Taylor microscales calculated for horizontal (λ_u) and vertical (λ_w) velocity components are 7mm and 9mm, respectively, again indicating privileged vertical direction.

4. NUMERICAL SIMULATIONS

A large series of numerical simulations, mimicking selected aspects of the cloud chamber experiment, have been performed (see Anrejczuk et al. 2004, 2006). The setup of these simulations was not aimed at the realistic repetition of the laboratory experiments which would be difficult due to the outflow from the chamber. Instead, simulations were intended to investigate key physical features of mixing, such as small-scale TKE generation by evaporative cooling at the edges of cloudy filaments and the role of droplet sedimentation in transport of cloud water across the cloud-clear air interface.

The model used in our simulations, referred to as EULAG, is described in Grabowski and Smolarkiewicz (2002) and in references cited there. Details of model equations, modeling setup, initial and boundary conditions as well as comprehensive discussion of various aspects of results are presented in Anrejczuk et al. (2004, 2006).

Herein, we only present relevant results from one of the simulations. It concerns a mixing event in the volume of $(64\text{cm})^3$ covered with 256^3 gridboxes (i.e., model grid length of 2.5mm). This corresponds to so-

called “coarsely resolved DNS” and requires no subgrid-scale parameterization (see discussion in Domaradzki et al. 2003).

We initialize the run with the prescribed analytical form of all fields (temperature, humidity, velocity, cloud water) representing a well-resolved pattern of cloud and clear air filaments, and look at the evolution of the mixing. The detailed parameterization of microphysics accounting for droplet sedimentation allows investigating evolution of droplet spectra and coupling between thermodynamics and microphysics. Initial temperature of the clear air is set to 293K and the relative humidity is 65%. Cloudy filaments are saturated, have the same temperature as the clear air, and have liquid water content (LWC) of 3.2g/kg. LWC content compensates the virtual temperature effect, which means that all buoyancy fluctuations in this particular simulation are due to the evaporation of cloud droplets and droplet sedimentation. This is different than in the cloud chamber experiment, where the plume was negatively buoyant due to the high LWC.

At the beginning of the simulation, the velocity field was isotropic with TKE set to $1.62 \cdot 10^{-4} \text{m}^2 \text{s}^{-2}$. In the first ten seconds of the simulation, the mean TKE increased from the initial value up to $2.2 \cdot 10^{-3} \text{m}^2 \text{s}^{-2}$ due to buoyant TKE production following droplet evaporation. From the 11th second, TKE decreased slowly due to prevailing dissipation. After 25 seconds of model time (the end of calculations), TKE was still about five times greater than its initial value, with the thermodynamic fields almost homogenized (see Anrejczuk et al. 2006).

Here we focus on anisotropy of the small-scale turbulence in the active stirring phase of the mixing, around $t=11$ sec. Fig. 4 shows the liquid water content field and the turbulent velocity fluctuation w' in the vertical cross-section through the computational domain. The figure shows filaments containing liquid water as well as patches of positive and negative vertical velocities elongated in the vertical.

As in the case of laboratory experiments, the horizontal Taylor microscale after 15 s of calculations ($\lambda_u=24\text{mm}$) is smaller than the vertical one ($\lambda_w=37$ mm). The ratio of the root mean square of turbulent velocity fluctuations: $\langle w'^2 \rangle / \langle u'^2 \rangle$ is 2.2 at that time, exactly like in the cloud chamber measurements. Distribution of turbulent velocity fluctuations (Fig 5, Table 2) is also similar: Gaussian with wider spread of vertical fluctuations than the horizontal.

TABLE 2. Distribution of horizontal (u' , v') and vertical (w') turbulent velocity fluctuations after 15s of calculations.

	Standard deviation [cm/s]	Skewness	Kurtosis
u'	3.19	-0.07	3.3
v'	3.09	-0.13	3.3
w'	4.56	0.15	3.0

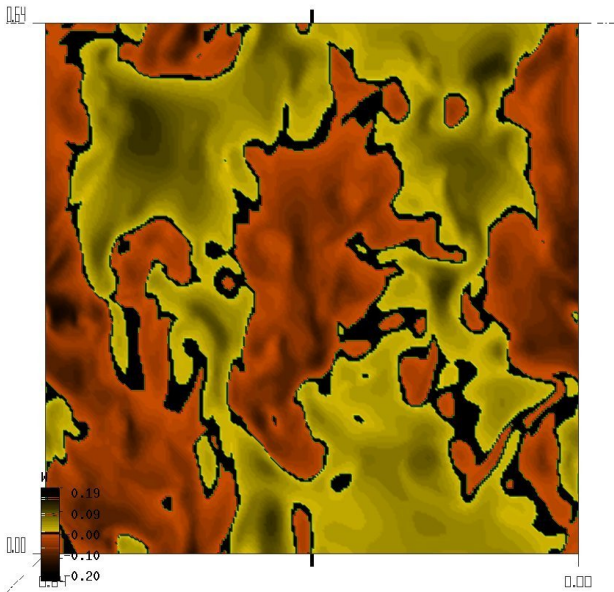
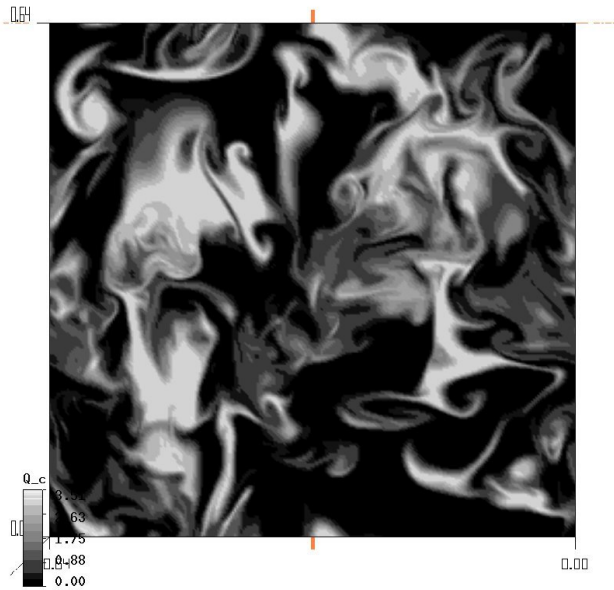


Fig.4. Liquid water content (upper panel) and vertical turbulent velocities (lower panel) on the XZ central section through the computational domain after 11s of simulations. Notice vertical elongation of structures in both panels.

Details:

Upper panel: bright areas represent cloudy filaments. Black areas represent clear filaments. A scale bar is in the left lower corner of the panel.

Lower panel: yellow areas represent positive values of the vertical component of turbulent velocity fluctuations, brown areas mark negative values. Color scale bar is in the left lower corner of the panel

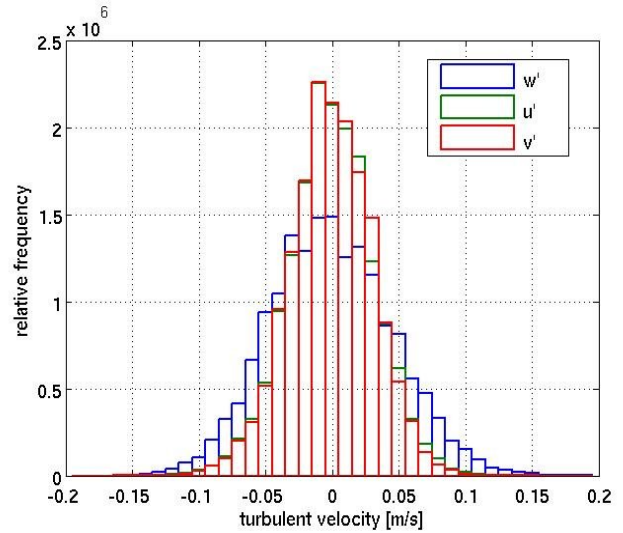


Fig.5. Distribution of horizontal (green u' and red v') and vertical (blue w') turbulent velocity fluctuations after 15s of simulations.

5. SUMMARY AND CONCLUSIONS

Small scale mixing of cloud with unsaturated environment is investigated in numerical simulations (spatial resolution of 2.5mm) and in laboratory cloud chamber experiments by means of Particle Image Velocimetry (PIV) with spatial resolution of 0.07mm. Despite substantial differences in physical conditions and various spatial resolutions (resolving well the dissipation scale in the laboratory and applying grid length larger than the Kolmogorov scale in the simulation), results of both investigations indicate that small-scale turbulence in such conditions is highly anisotropic with the preferred direction in the vertical. Buoyancy forces resulting from evaporation of cloud droplets substantially influence smallest scales of turbulence. The vertical direction, in which buoyancy force acts, is preferred. Typically, $\langle (u')^2 \rangle$ is about two times smaller than $\langle (w')^2 \rangle$. The probability distribution functions of w' are wider than those of u' . It is still uncertain to what extent these results apply to real clouds. In situ measurements of turbulent velocity fluctuations from various types of clouds are necessary to validate common assumptions of small-scale cloud isotropy.

ACKNOWLEDGMENTS

This work was supported by the Polish Ministry of Science and Higher Education, by NCAR's Clouds in Climate and Geophysical Turbulence programs and by the European Union under grant EVK2-CT2002-80010-CESSAR. NCAR is sponsored by the National Science Foundation.

REFERENCES:

- Andrejczuk, M., W. W. Grabowski, S. P. Malinowski and P. K. Smolarkiewicz, 2004: Numerical simulation of cloud-clear air interfacial mixing. *J. Atmos. Sci.*, **61**, 1726-1739.
- Andrejczuk, M., W. W. Grabowski, S.P. Malinowski and P.K. Smolarkiewicz 2006: Numerical Simulation of Cloud-Clear Air Interfacial Mixing: Effects on cloud- microphysics *J. Atmos. Sci.*, in press.
- Banat, P. and S. P. Malinowski, 1999: Properties of the turbulent cloud-clear air interface observed in the laboratory experiment. *Phys. Chem. Earth (B)*, **24**, 741-745.
- Broadwell, J. E., and R. E. Breidenthal, 1982: A simple model of mixing and chemical reaction in a turbulent shear layer. *J. Fluid Mech.*, **125**, 397–410.
- Domaradzki, J.A., Z.Xiao and P.K. Smolarkiewicz, 2003: Effective eddy viscosities in implicit modelling of turbulent flows. *Phys. Fluids*, **15**, 3890-3893.
- Falkovich G., K. Gawedzki and M. Vergassola, 2001, Particles and fields in fluid turbulence. *Rev. Modern Phys.*, **73**, 913-975.
- Ghosh, S., Davila, J., Hunt, J.C.R., Srdic, A., Fernando, H.J.S. and Jonas P.R., 2005, How turbulence enhances coalescence of settling particles with applications to rain in clouds, *Proc R. Soc. A*, **461**, 3059-3088.
- Grabowski W. W., 1993: Cumulus entrainment, fine-scale mixing and buoyancy reversal. *Quart. J. Roy. Met. Soc.*, **119**, 935-956.
- Grabowski, W.W. and P. K. Smolarkiewicz, 2002: A multiscale model for meteorological research. *Mon. Wea. Rev.*, **130**, 939–956.
- Korczyk, P. M., S. P. Malinowski and T. A. Kowalewski, 2006: Mixing of cloud and clear air in centimeter scales observed in laboratory by means of particle image velocimetry. *Atmos. Res.* in press.
- Malinowski, S. P., and I. Zawadzki, 1993: On the surface of clouds. *J. Atmos. Sci.*, **50**, 5–13.
- Malinowski, S. P., I. Zawadzki and P. Banat, 1998: Laboratory observations of cloud clear air mixing in small scales. *J. Atmos. Oceanic Technol.*, **15**, 1060-1065.
- Malinowski, S.P. and A. Jaczewski, 1999: Laboratory investigation of the droplet concentration at the cloud-clear air interface. *Phys. Chem. Earth B*, **24**, 477-480.
- Shaw R.A., 2003, Particle-turbulence interactions in atmospheric clouds, *Bull. Amer. Meteorol. Soc.*, **35**, 183-227.
- Siebert, H., K. Lehmann and M. Wendisch, 2006: Observations of Small Scale Turbulence and energy Dissipation Rates in Cloudy Boundary Layer. *J. Atmos. Sci.*, in press.
- Vaillancourt, P.A. and M. K. Yau, 2000: Review of particle-turbulence interactions and consequences for cloud physics. *Bull. Amer Meteorol. Soc.*, **81** (2): 285-298.